SP2 Report on

Reactions of CAC in the Field
Hydration, Conversion, Carbonation and Corrosion

Part 2: XRD and SEM/EBSD Analysis

Author and Chief Investigator: M. Valix

Summary

The X-ray diffraction and SEM/EBSD analyses were conducted to complement the thermal analysis of the 6 year CAC cores obtained from Hayden Pl. Banksmeadow. The following conclusions were derived from these analyses:

- Hydration of CA does not appear to be complete at the installation of CAC. CA hydration appear to continue with time at a very slow rate depending on the availability of moisture. CA hydration was found to be greater at the sewer front than closer to the concrete. Although it appears higher in the wall, then tidal then roof.
- The implication of an incomplete hydration is that the hydration reaction will continue to feed CAC with unstable phases that are continually converted. The overall result is the accumulation of both unstable and stable phases. This is evident when comparing the higher AH_3 and C_3AH_6 peaks after many years of service with CAC that is fully converted at 100°C. Despite having immediately converted all the unstable phase 100°C, with time more unstable phases are formed eventually leading to much higher AH_3 and C_3AH_6 peaks.
- The accumulation of the higher AH_3 and C_3AH_6 peaks with time suggests the corrosivity in these Sydney sewer sites is low.
- The conversion at the sewer front is higher and progressively reduced as CAC moves towards the concrete side. This is attributed to again higher moisture content on the sewer front resulting in higher hydration reaction. Although the sewer front shows 80% conversion, it is apparent the CAC closer to the concrete has conversion similar to the point of installation.
- Examination of the CAC hydrate reveals the preferential corrosion of C_3AH_6. The removal of C_3AH_6 is higher in the roof that on the wall and tidal zone. This is attributed to both corrosion and carbonation of C_3AH_6. The effect of carbonation was shown in the thermal analysis of CAC. Carbonation converts CAC to $CaCO_3$ resulting in the reduction of pH to about 7.5-8.0. The reduction in alkalinity means it will have lower resistance to acid attack. Thus it appears corrosion on the roof is higher than the tidal or wall. $CaCO_3$ was not observed in the XRD analysis, it is presumed this phase is amorphous.
- In terms of the unstable phases, it appears brownmillerite (C_2AFH_8) is preferentially formed instead of mayenite C_2AH_8. The brownmillerite and stratlingite phases demonstrate greater resistance to corrosion compared to C_3AH_6.
- Although our biogenic analysis showed both organic acids and small quantities of sulphuric acid, only the sulphuric acid corrosion product (ettringite, $C_6A_2S_3H_{32}$) was observed in the CAC sample. This could be attributed to the high solubility of Al-citrate complexes. Ettringite was observed to form across the CAC sample from 0-1 to 3-4 cm layers in the roof, wall and tidal zone. This would suggest that sulphuric acid has permeated through the whole CAC sample.
- CAC was also observed to expand. The expansion for the 6 year field sample was more difficult to assess. Field samples of coupons that have been installed in the Sydney sewers were included in this report instead, demonstrating the expansion of CAC during service.

It is apparent that expansion does not occur immediately but it appears to occur significantly after 300- 500 days. The expansion appears to occur as a result of changes in the density of the CAC hydrates and corrosion products. The formation of brownmillerite, which has a very high density of 3684 (kg/m^3) appears to contribute to the expansion. Its conversion to the lower density C_3AH_6 (2529 kg/m^3) and AH_3 (2420 kg/m^3) results in CAC expansion. The expansion however is also greater with the formation of stratlingite (or hydrated gehlenite) that has a density of 1940 kg/m^3 and ettringite that has a 1775 kg/m^3.

1.0 Hydration Reactions

The hydration reaction, as suggested from the first part of this report, feeds the CAC with the metastable phases and these in turn are converted to the stable C_3AH_6 and the AH_3. The cyclic progression of these reactions results in the accumulation of C_3AH_6 and the AH_3.

In this section of the analysis, we confirm the progression of the hydration reaction using X-ray diffraction. The mineral krotite ($CaOAl_2O_3$) has its highest intensity around 30.1°(Horkner and Mullerbuschbaum 1976). This theta spacing was used to analyse the unhydrated calcium aluminate (CA) remaining in the CAC obtained from the field. Figure 1 shows the CA phase for 4 specimen and demonstrate the progressive hydration in the field. The highest peak height belongs to the CAC that is cured after 28 days and this is followed 2 year field and 6 year field CAC samples obtained from Sydney water SWSOOS 2 sewers. Finally the least peak height results from the aggressive corrosion of CAC at 45°C with 1 M H_2SO_4. The 2 year and 6 years.

These results show that the hydration reaction is not complete at the installation of CAC but it progressively continues over a period of time whilst still in service. The small change from 2 to 6 years suggest that hydration reaction becomes very slow and this could be attributed to the small quantity of water available to the CA.

The broadening of the CA peak suggests anisotropic strain resulting from the transformation from crystalline to amorphous CA structure.

The overall result on the hydrated phased is shown in Figure 2. The green peak associated with CAC rapidly cured at 100°C would be presumed to be the maximum if all the CA are hydrated. However as shown the C_3AH_6 and the AH_3 continued to progressively increase with time. The reduction of these two phases was also observed and this was attributed to corrosion and carbonation reaction.

Figure 3 shows that extent of hydration is higher closer to the sewer front than CAC found that is progressively closer to the concrete substrate.

Figure 4 shows the extent of hydration is greater on the wall than it is on the roof and tidal zone. This appears to contradict the effect of higher moisture on the tidal zone.

The effect of environmental conditions on the hydration reaction is shown in Figure 5. There is no significant difference in the CA peak heights with conditions with the exception of Melbourne. Only corrosion products and stratlingite were found in the Melbourne CAC.

The implication of an incomplete hydration is that the hydration reaction will continue to feed CAC with unstable phases that are continually converted. The overall result is the accumulation of both unstable and stable phases. This is evident when comparing the higher AH_3 and C_3AH_6 peaks after many years of service with CAC that is fully converted at 100°C. Despite having immediately converted all the unstable phase 100°C, with time more unstable phases are formed eventually leading to much higher AH_3 and C_3AH_6 peaks.

It appear that controlling the cement to water ratio has a significant effect in controlling the hydration reaction and thus the long term performance of CAC.

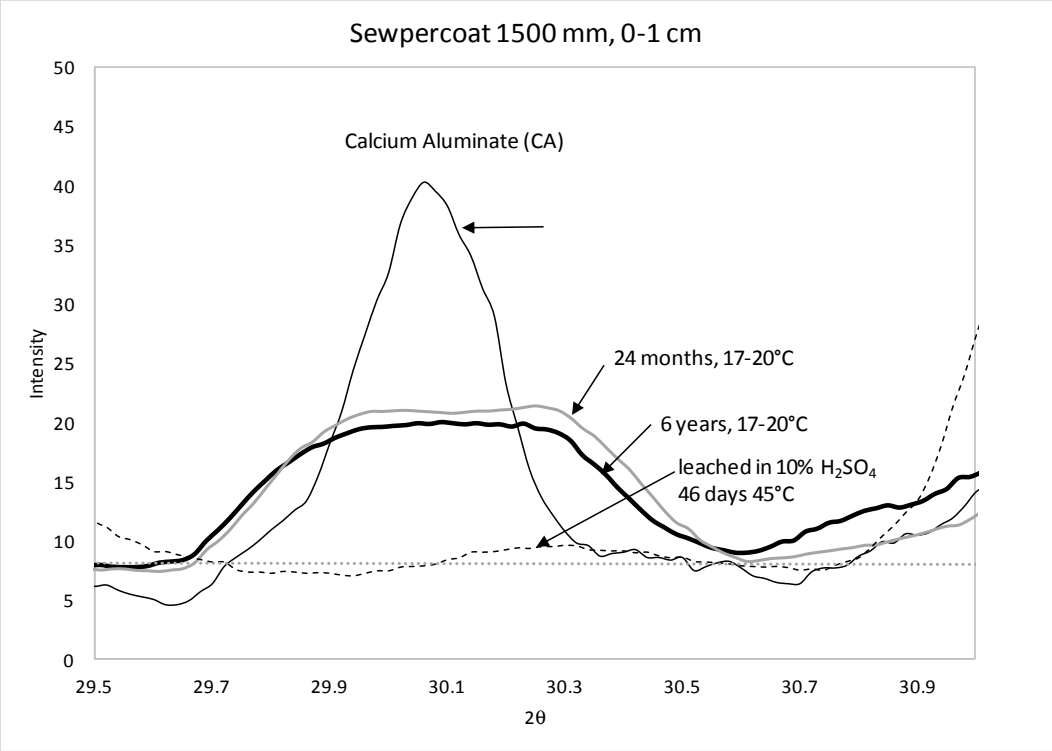

Figure 1. Hydration of CAC with time.

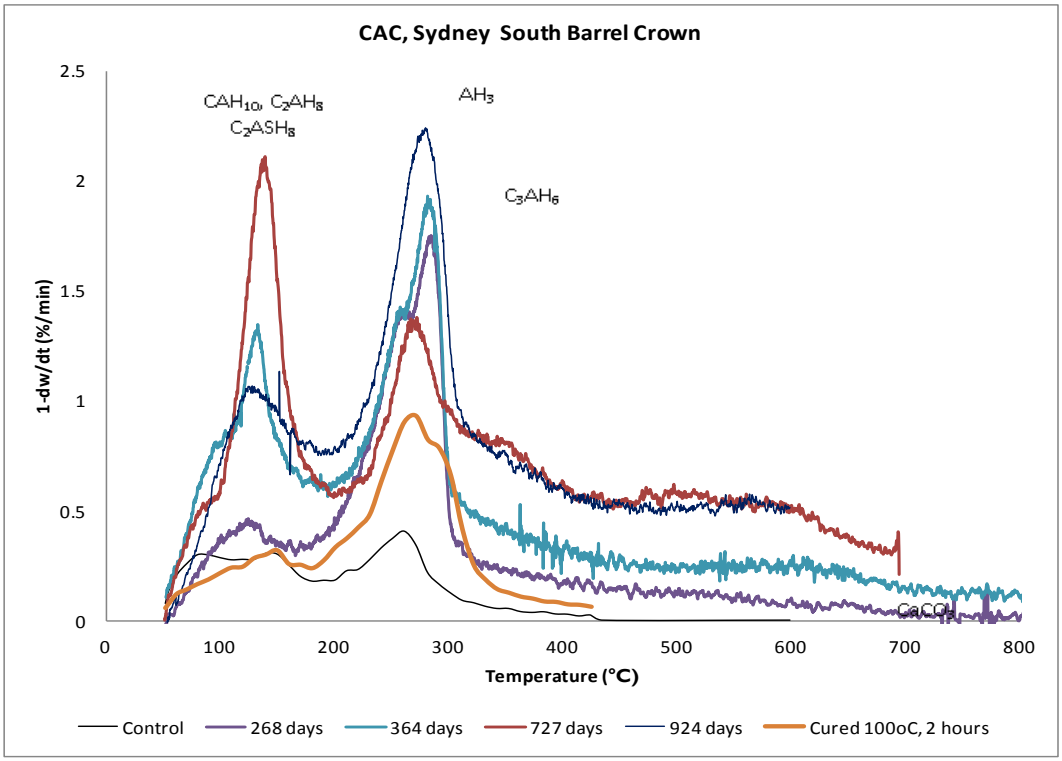

Figure 2. DTG of CAC installed in the crown of Sydney SWSOOS South Barrel sewer (4.27 ppm H_2S, 20.5°C, 97.7% RH). The control was cured for 24 hours at 99% relative humidity at 21°C.

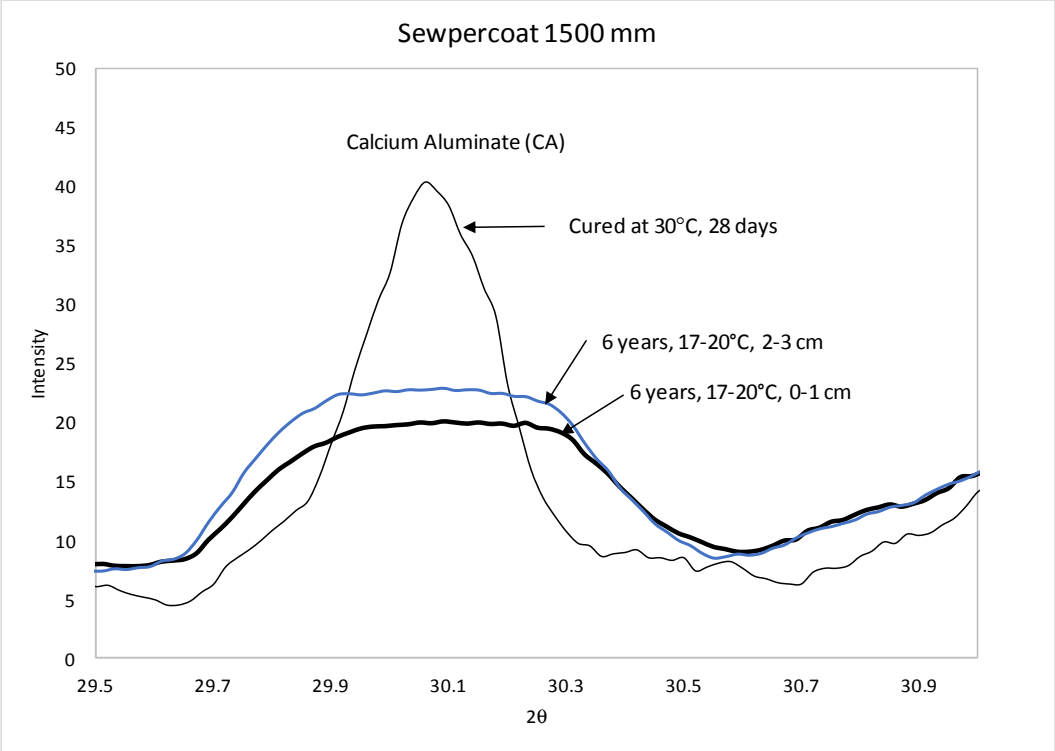

Figure 3. Hydration across the CAC sample from the sewer face (0-1 cm) through to the concrete (2-3 cm).

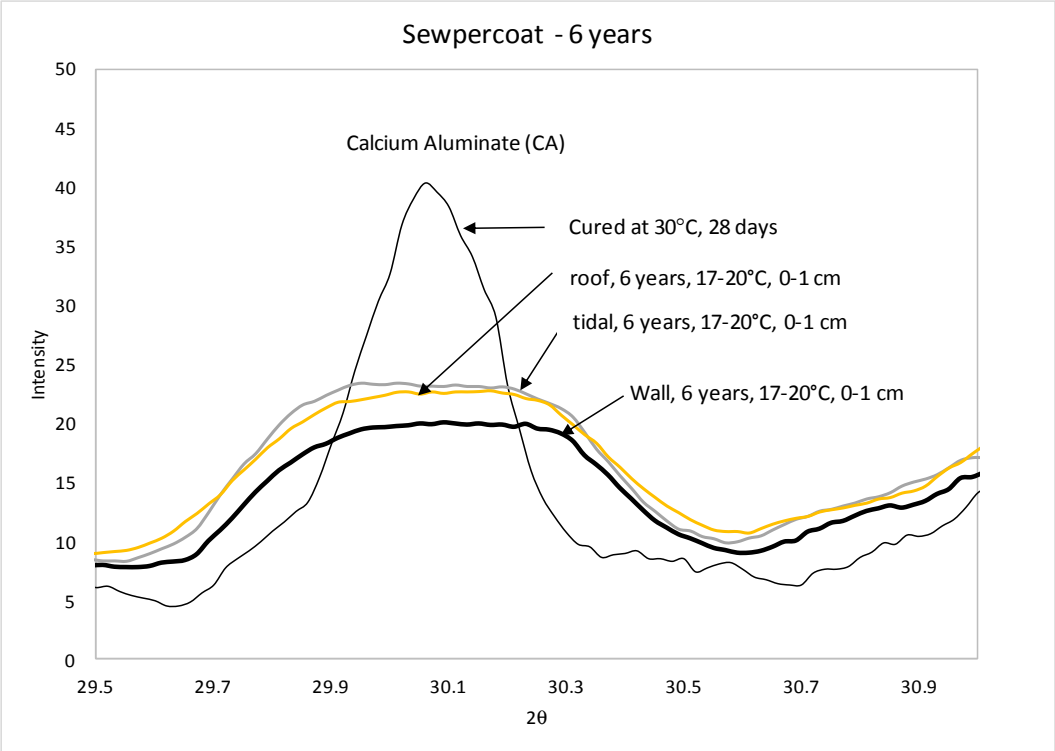

Figure 4. Extent of hydration as a function of location in CAC after 6 years of service.

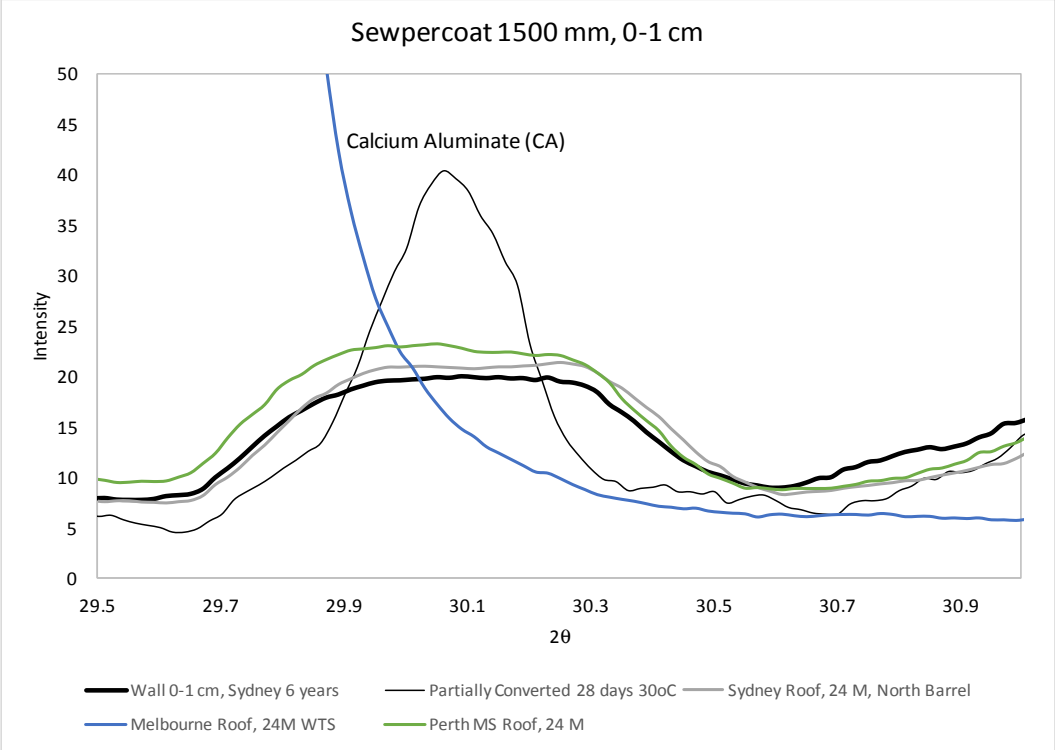

Figure 5. The hydration as a function of H_2S concentration (Sydney: 3-5 ppm, Melbourne 4-10 ppm and Perth 100-800 ppm).

1.2 Conversion and Corrosion Across the Coating

The conversion to the stable phase (C_3AH_6) across the 6 year CAC coating is shown in Figure 6. As shown the stable phase progressively increases from the sewer front towards the concrete substrate. The relatively lower value close to the sewer front confirms its preferential corrosion. Its complete depletion on the roof could be attributed to both corrosion and to its carbonation, that was demonstrated from the thermal analysis presented in the first part of this report.

These results demonstrate that there is still substantial amount of the stable phase C_3AH_6 remaining after 6 years of service, particularly closer to the concrete.

In contrast, the remaining unstable phases are shown in Figure 7. Here only mayenite (C_2AH_8) and potentially brownmillerite ($C_2(AF)H_8$) are still quite prominent on the CAC sample after 6 years of service. The 2q d spacing for both mayenite and brownmillerite are quire similar and are difficult to distinguish. It is apparent that the unstable phase decreases as it moves towards the concrete. However in the roof, its relative difference from the 0-1 cm layer compared to the 2-3 cm and 3-4 cm is slightly higher. This could be attributed to the greater corrosion in the roof. The progressive decline across the coating suggest its greater resistance to acid attack. That is once the C_3AH_6 and AH_3 are removed preferentially by corrosion, it appears the unstable phase remains.

The formation of stratlingite across the CAC coating showed similar trend to the unstable phase in Figure. That is there is progressive reduction as it moves towards the concrete phase. Again this could be attributed to its resistance to acid attack.

Although our biogenic analysis showed both organic acids and small quantities of sulphuric acid, only the sulphuric acid corrosion product (ettringite, $C_6A_2S_3H_{32}$) was observed in the CAC sample. This could be attributed to the high solubility of Al-citrate complexes.

The formation of ettringite results from the sulfate attack of CAC hydrates (Evju and Hansen 2001, Nocun-Wczelik et al. 2011, Tixier and Mobasher 2003, Zuo et al. 2012). This reaction begins with the sulfate attack of $Ca(OH)_2$(O'Connell et al. 2010):

$$Ca(OH)_2 + H_2SO_4 \rightarrow CaSO_4 + 2H_2O \quad (1)$$

The hydrated $CaSO_4$ form gypsum, which attacks the stable phase C_3A:

$$C_3A + 2CaSO_4.2H_2O + 2Ca(OH)_2 + 26H_2O = C_3A.3CaSO_4.32H_2O \quad (2)$$

The formation of ettringite across the CAC demonstrate the acid permeation has occurred through the CAC coating.

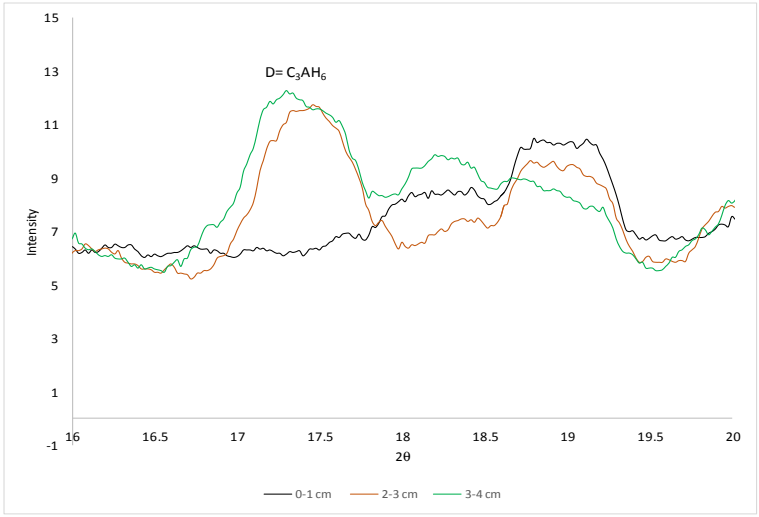

Roof

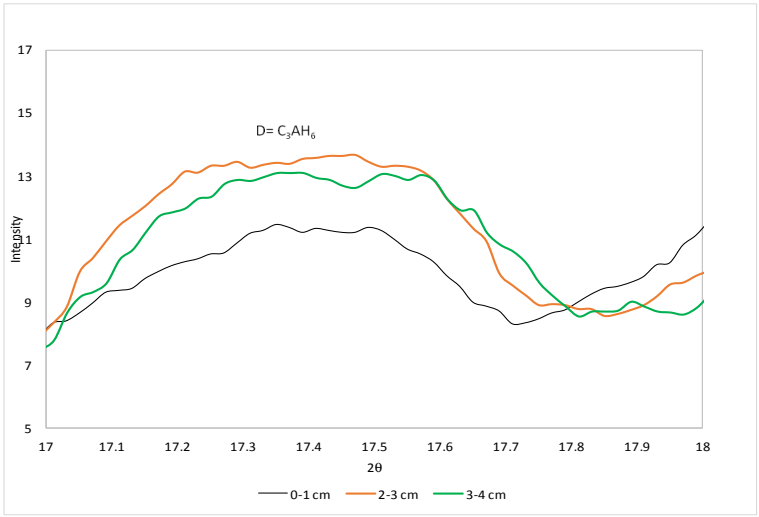

Wall (1500 mm from the sewage floor)

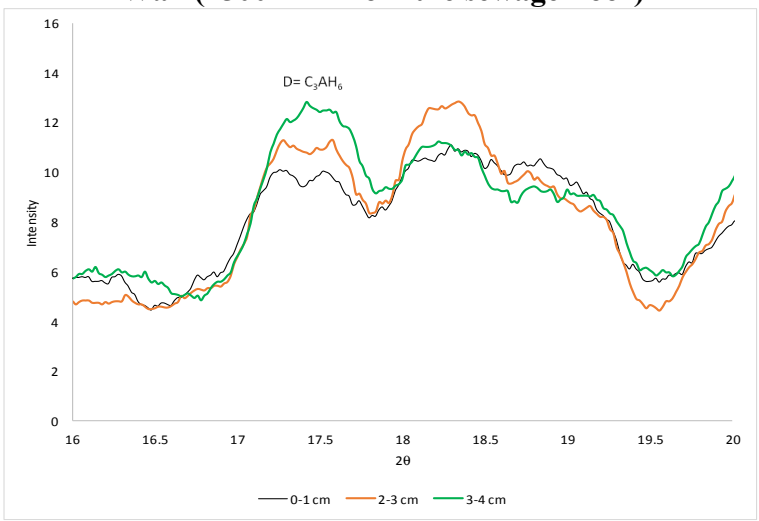

Tidal zone (1000 mm from the sewage floor)

Figure 6. Conversion to C_3AH_6 across the CAC coating at various location for CAC (6 years service)

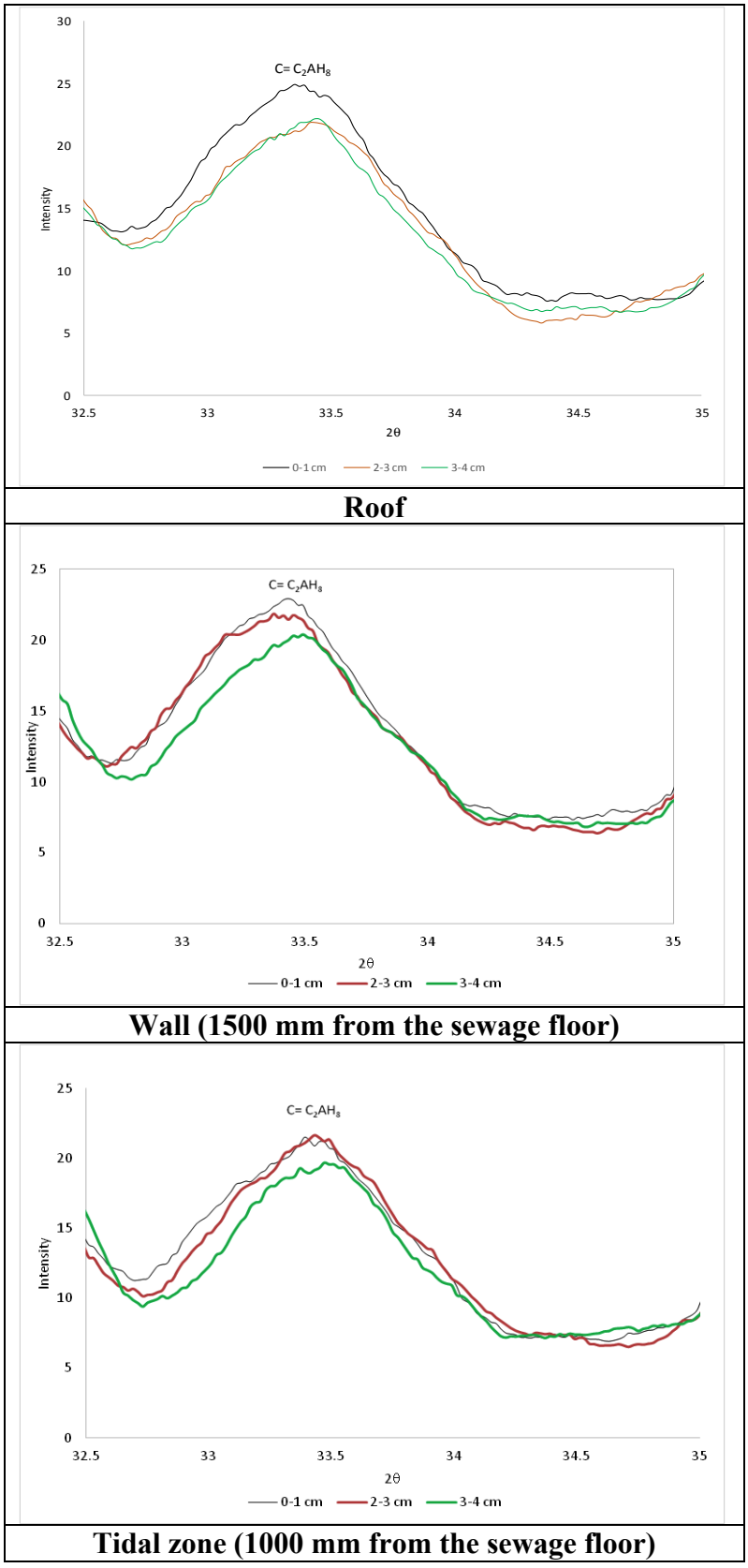

Figure 7. Unconverted (C_2AH_8) and ($C_2(AF)H_8$) across the CAC coating at various location for CAC (6 years service)

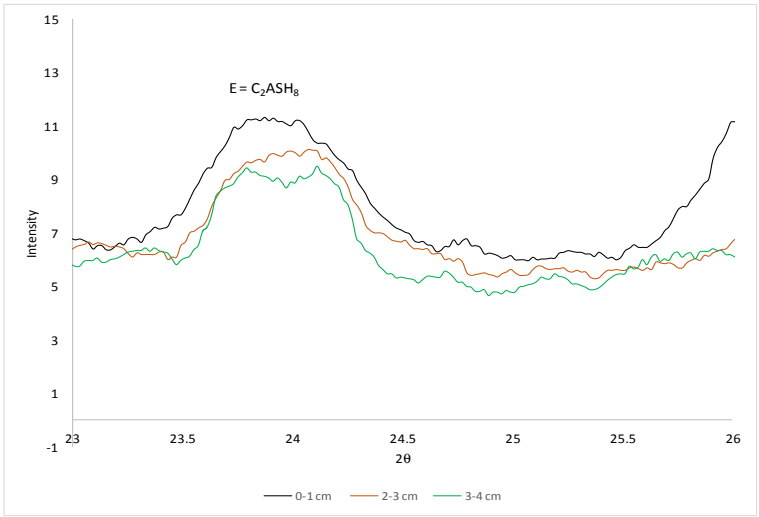

Roof

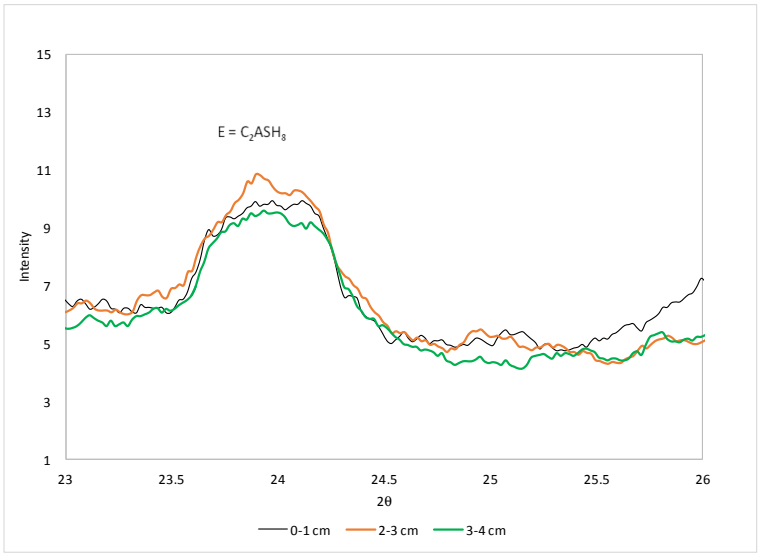

Wall (1500 mm from the sewage floor)

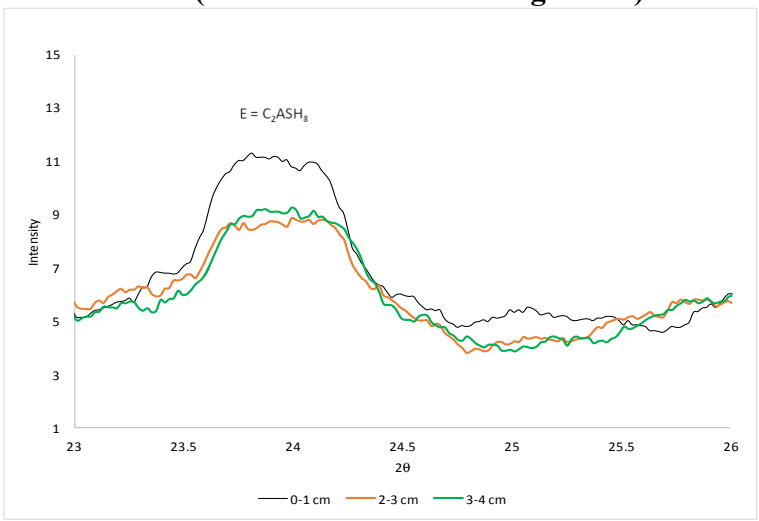

Tidal zone (1000 mm from the sewage floor)

Figure 8. Stratlingite (C_2ASH_8) across the CAC coating at various location for CAC (6 years service)

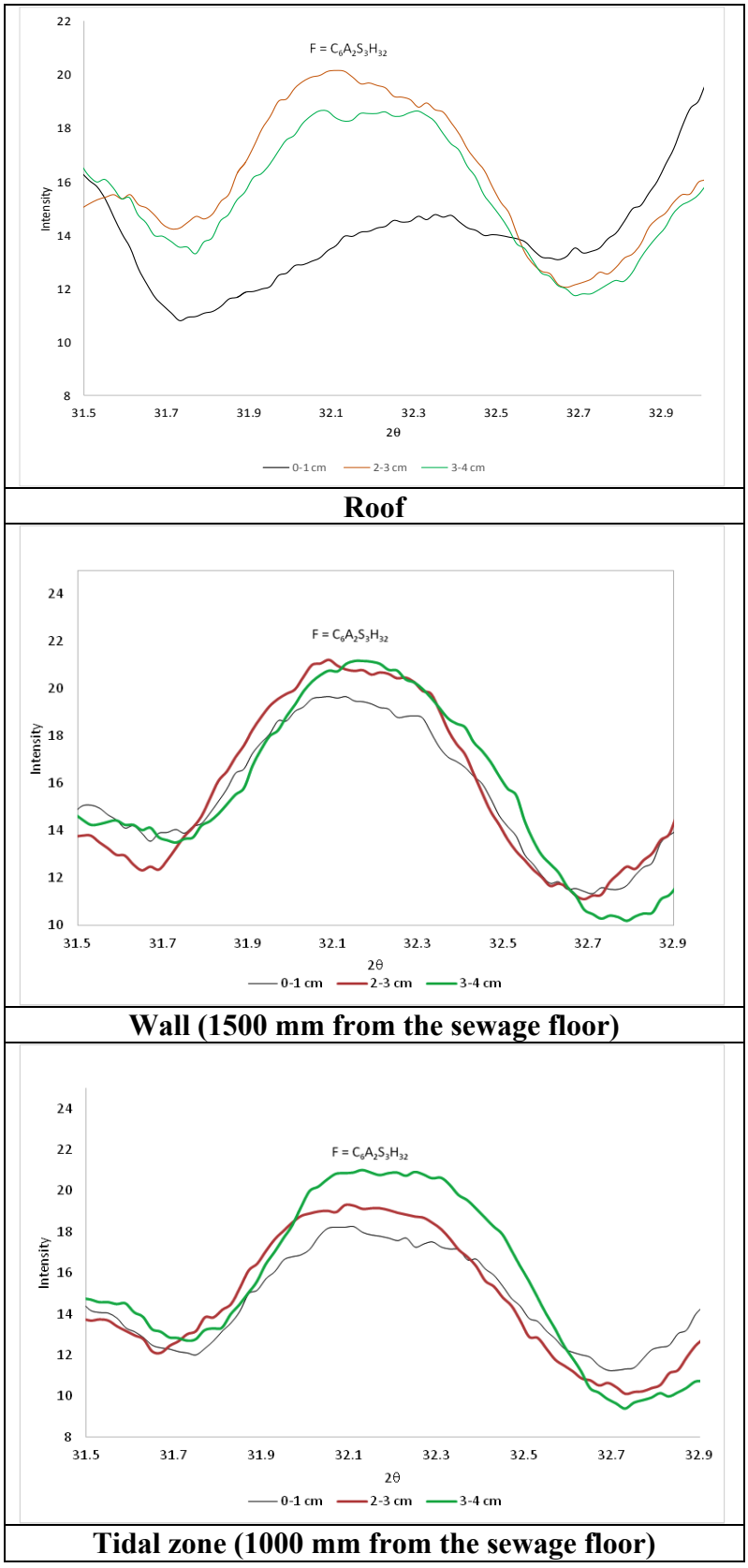

Figure 9. Ettringite ($C_6A_2S_3H_{32}$) formation across the CAC coating at various location for CAC (6 years service)

1.3 CAC Expansion

A feature that was observed in CAC coupons installed in Sydney Water sewers for 30 months is the expansion. Figure 10 demonstrate both the corrosion (loss of thickness) but also expansion (increase in thickness of CAC. At the early phase it is apparent the coupons are losing thickness consistent with corrosion. However at the later stage of the installation, the coupons consistently showed an expansion, followed by further corrosion. Expansion of coupons installed in the crown appears to occur at 553 days in North barrel and 727 days in the South barrel. Greater expansion is observed in the North barrel than in the South barrel. In the tidal zone, the expansion occurred earlier, at 268 days.

The expansion of CAC would ultimately lead to increased porosity and greater accessibility of the corroding acid. This feature is likely to have an impact on the rate of corrosion of CAC.

In this aspect of this analysis, the aim is to establish the reason for the expansion of CAC. Various factors can contribute to the shrinkage and expansion of CAC. In this study it appears to be attributed to the changes in the density of the CAC hydrates and corrosion products.

The higher density means lower volume and would result in shrinkage of the solids. While lower density means higher volume and should result in expansion. Table 1 shows the density of the various CAC hydrates and corrosion product.

The formation of metastable and stable phases results in the chemical shrinkage of CAC (Fu 2011, Ideker 2008). As shown in Table 1 this results from the higher density of the metastable and stable phases relative to CAH_{10}.

Table 1. Density of CAC hydrates and Corrosion product

Type of Mineral	**CAC Phases**	Density (kg/m^3)	References
Metastable CAC Hydrates	CAH_{10}	1720	(Parr 2004)
	α-C_2AH_8	1950	(Scheller 1974)
	β-C_2AH_8	1950	(Scheller 1974)
	Brownmillerite $C_2(AF)H_8$	3684	(Colville and Geller 1971)
Stable CAC Hydrate	C_3AH_6	2529	(Lager et al. 1987)
	$Al(OH)_3$	2420	Web mineral
	Stratlingite C_2ASH_8	1940	(Kuzel 1976)
Corrosion Product	Ettingrite ($C_6A\ S_3H_{32}$)	1775	(Struble 1986)

The EBSD analysis of CAC partially converted at 28 days at 30°C reveals principally the unstable phases CAH_{10}, brownmillerite ($C_2(AF)H_8$) and gehlenite (unhydrated stratlingite). An iron spinel was also observed (see Figure 11). The corresponding phase

fraction analysis is shown in Table 2. A similar analysis of CAC with 5% Fly Ash converted at 100°C showed similar analysis in Figure 12. The phase fraction analysis in Table 3 reveals a higher fraction of gehlenite (25%) is formed with 5% fly ash compared to CAC without additional fly ash (19.9%), however the brownmillerite fraction also increased.

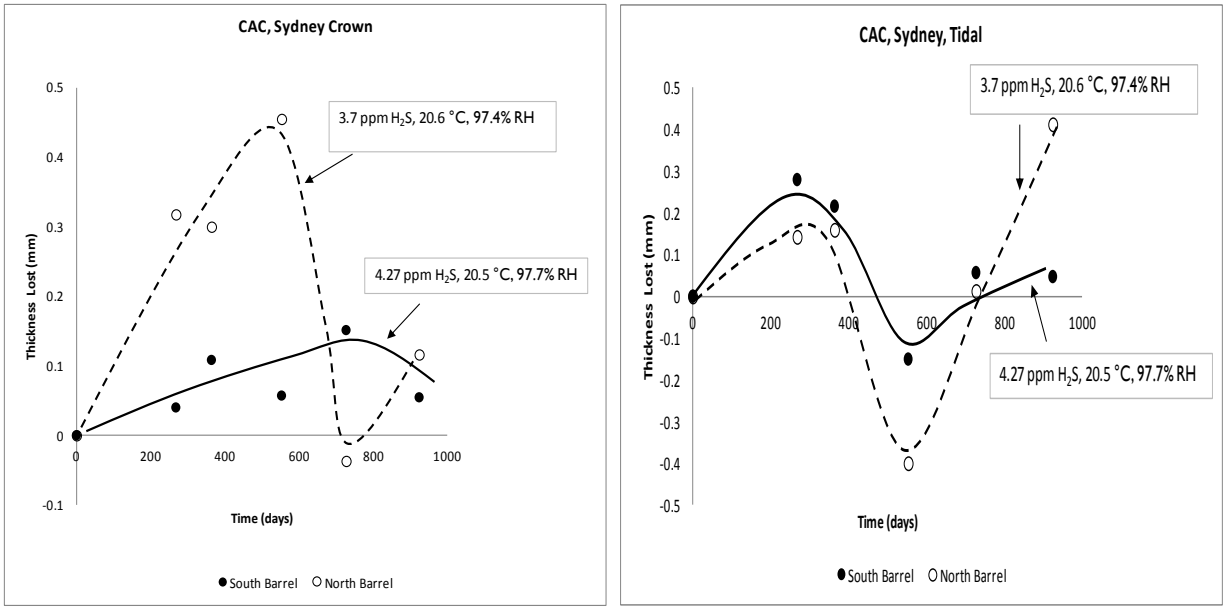

(a) (b)

Figure 10. Rate of corrosion of calcium aluminate cement in the a) crown and b) tidal zpne of Sydney sewers.

The observed expansion of CAC observed in Figure 10 appear to result from the formation of brownmillerite which has an exceptionally higher density compared to mayenite (C_2AH_8). Brownmillerite is similar to mayenite (C_2AH_8) but some of Al is replaced with Fe to form $C_2(AF)H_8$. Brownmillerite, which has a density of 3684 (kg/m^3) and when converted to lower density C_3AH_6 (2529 kg/m^3) and AH_3 (2420 kg/m^3) would result in CAC expansion. The expansion would also be greater with the formation of stratlingite (or hydrated gehlenite) that has a density of 1940 kg/m^3. Figures 11 and 12 confirm its formation.

The formation of corrosion product ettringite that has a 1775 kg/m^3 would also result in CAC expansion. The XRD results in Figure 9 confirm its formation.

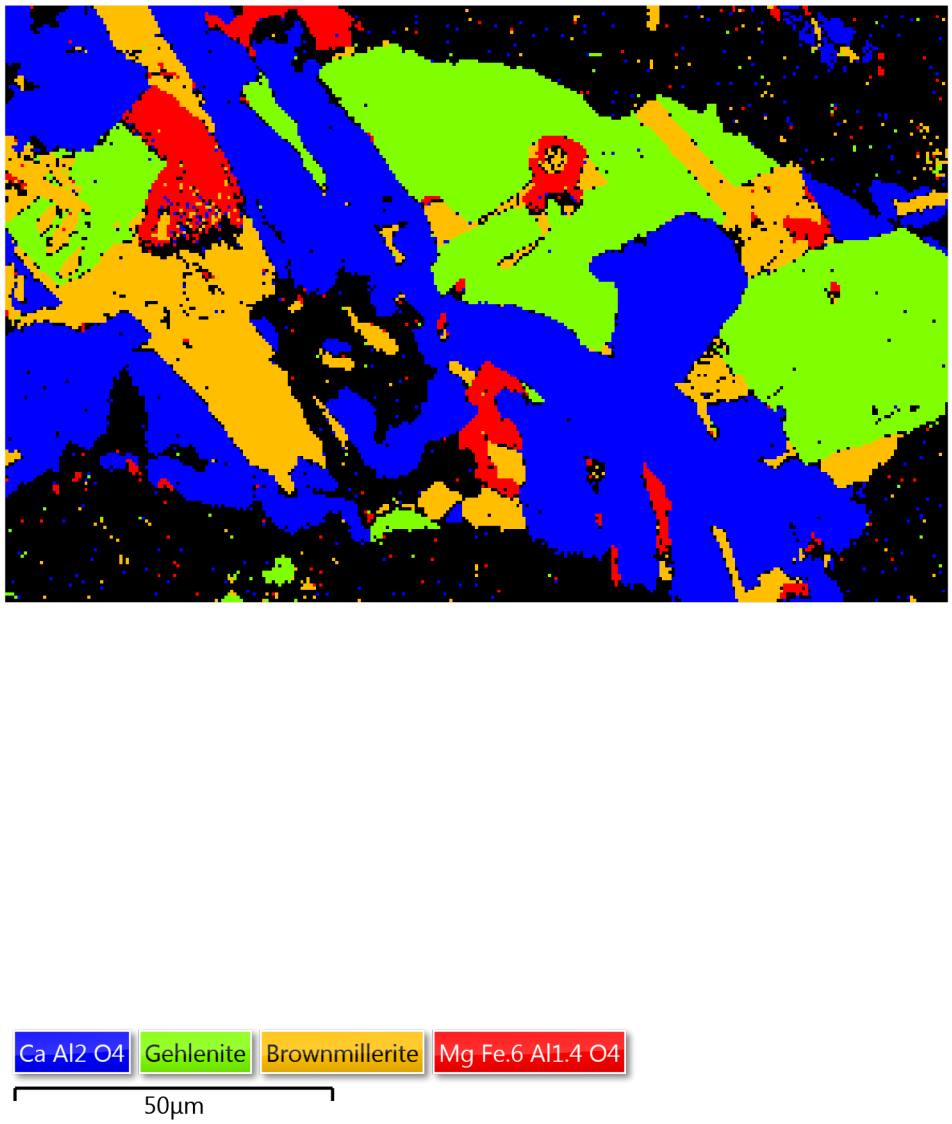

Figure 11. EBSD Analysis of CAC Partially Converted for 28 days at 30°C.

Table 2. Phase Fraction Analysis of CAC Partially Converted for 28 days at 30°C.

Phase Name	Phase Fraction (%)	Phase Count
Ca Al2 O4	32.24	18000
Gehlenite	19.75	11026
Brownmillerite	12.07	6740
Mg Fe.6 Al1.4 O4	4.32	2412
Zero Solutions	31.62	17654

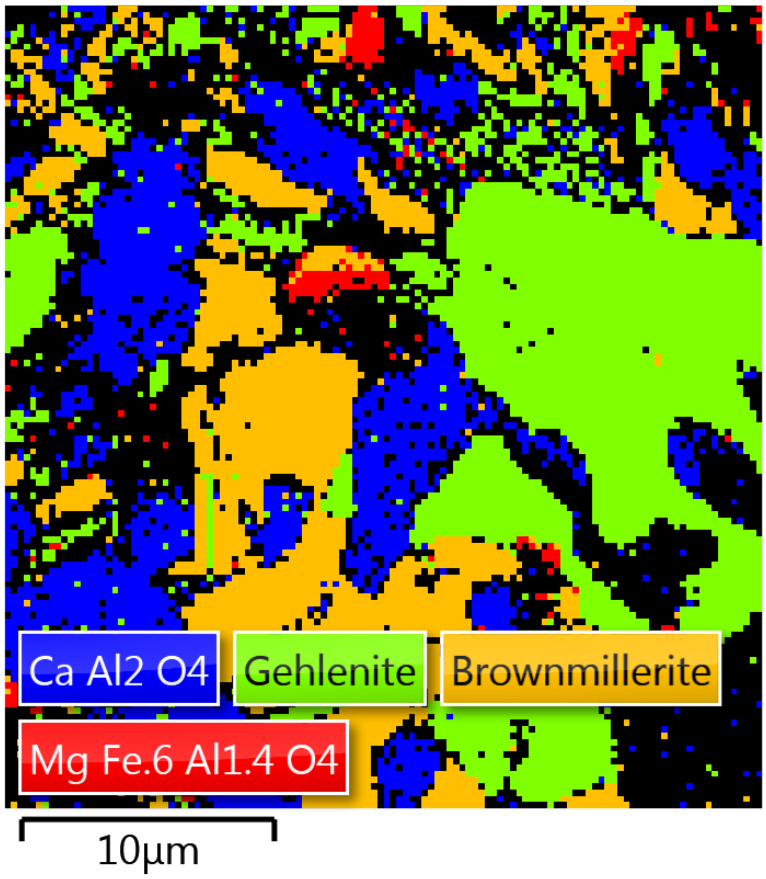

Figure 12. EBSD Analysis of CAC + 5% Fly Ash Converted at 100°C.

Table 3. Phase Fraction Analysis of CAC Partially Converted for 28 days at 30°C.

Phase Name	Phase Fraction (%)	Phase Count
Ca Al2 O4	18.53	2824
Gehlenite	25.28	3853
Brownmillerite	18.79	2864
Mg Fe.6 Al1.4 O4	1.58	241
Zero Solutions	35.81	5458

References

1. Colville AA, Geller S. 1971. CRYSTAL STRUCTURE OF BROWNMILLERITE, CA2FEALO5. Acta Crystallographica Section B-Structural Crystallography and Crystal Chemistry B 27: 2311-&.
2. Evju C, Hansen S. 2001. Expansive properties of ettringite in a mixture of calcium aluminate cement, Portland cement and beta-calcium sulfate hemihydrate. Cement and Concrete Research 31: 257-261.
3. Fu T. 2011. Autogenous Deformation and Chemical Shrinkage of High Performance
4. Cementitious SystemsOregon State University.
5. Horkner W, Mullerbuschbaum HK. 1976. CRYSTAL-STRUCTURE OF CAAL2O4. Journal of Inorganic & Nuclear Chemistry 38: 983-984.
6. Ideker JH. 2008. Early-Age Behavior of Calcium Aluminate Cement SystemsThe University of Texas at Austin.
7. Kuzel HJ. 1976. Neues Jahrbuch für Mineralogie Monatshefte 319-325
8. Lager GA, Armbruster T, Faber J. 1987. NEUTRON AND X-RAY-DIFFRACTION STUDY OF HYDROGARNET CA3AL2(O4H4)3. American Mineralogist 72: 756-765.
9. Nocun-Wczelik W, Konik Z, Stok A. 2011. Blended systems with calcium aluminate and calcium sulphate expansive additives. Construction and Building Materials 25: 939-943.
10. O'Connell M, McNally C, Richardson MG. 2010. Biochemical attack on concrete in wastewater applications: A state of the art review. Cement & Concrete Composites 32: 479-485.
11. Parr C, Simonin, F., Touzo, B., Wohmeyer, C., Valdelievre, B., Namba, A., . 2004. The impact of Calcium Aluminate cement hydration upon the properties of refractory castables. Paper presented at TARJ MEETING; 30 September 2004 AKO, JAPAN.
12. Scheller T, Kuzel, H. J. . 1974. Studies on dicalcium aluminate hydrates. Paper presented at The 6th International Congress on the Chemistry of Cement,, Moscow.
13. Struble LJ. 1986. 8th International Congress on the Chemistry of Cement. Pages 582-588.
14. Tixier R, Mobasher B. 2003. Modeling of damage in cement-based materials subjected to external sulfate attack. I: Formulation. Journal of Materials in Civil Engineering 15: 305-313.
15. Zuo XB, Sun W, Yu C. 2012. Numerical investigation on expansive volume strain in concrete subjected to sulfate attack. Construction and Building Materials 36: 404-410.